

# {311} defect evolution in ion-implanted, relaxed Si<sub>1-x</sub>Ge<sub>x</sub>

Robert Crosby,<sup>a)</sup> K. S. Jones, and M. E. Law  
*University of Florida, SWAMP Group, Gainesville, Florida 32611*

A. Nylandsted Larsen and J. Lundsgaard Hansen  
*Institute of Physics and Astronomy, University of Aarhus, DK-8000, Aarhus, Denmark*

(Received 1 June 2003; accepted 25 August 2003; published 4 February 2004)

Si-implanted, unstrained Si<sub>1-x</sub>Ge<sub>x</sub> layers of various Ge concentrations ranging from 0% to 50% were grown by molecular beam epitaxy on top of a Si substrate. The samples were subjected to a 750 °C anneal for 180 min to explore the subsequent defect structure. Plan-view transmission electron microscopy was implemented to investigate the evolution of defects. The Si<sub>1-x</sub>Ge<sub>x</sub> samples with ≤5% Ge exhibit {311} defect formation and dissolution, and these defects ripen throughout the course of the anneal. Increasing the Ge content has an adverse effect on the growth of {311} defects. The samples with Ge contents ≥25% demonstrated only dislocation loop formation. Dislocation loop formation and the observed impedance of {311} defect growth is facilitated by increasing the Ge content due to the weak bonding associated with the Ge atoms. © 2004 American Vacuum Society. [DOI: 10.1116/1.1619423]

## I. INTRODUCTION

Heterostructures via Si<sub>1-x</sub>Ge<sub>x</sub> alloys are attractive to the semiconductor industry and have been utilized in countless electronic device applications<sup>1-3</sup> due to the simplicity of band gap engineering<sup>4</sup> and the Hume-Rothery agreement between Si and Ge. Hence a great deal of scientific attention has been concentrated in understanding the physical nature of these alloys.

Ion implantation is the most effective method of doping Si for semiconductor device applications due to its precise dose and directional control. Annealing is necessary to correct the implantation damage and activate the dopants. During the anneal, the displaced ions may undergo transient enhanced diffusion (TED) resulting from the movement of excess interstitials residing in the damaged region.<sup>5</sup> Depending on implant and annealing conditions, {311} defects and dislocation loops may form near the projected range of the implant where supersaturation is the highest<sup>6,7</sup> due to the motion of these interstitials. Discernible by transmission electron microscopy (TEM), the “rod-like” {311} defects are a monolayer of hexagonal interstitials based in the {311} habit planes.<sup>8</sup> Upon annealing, these {311} defects are known to act as a sink for interstitials and coarsen.<sup>5</sup> In the latter stages of the anneal, the {311} defects will unfault, form dislocation loops, and then release the interstitials that lead to TED.<sup>5,9,10</sup> Following the use of Si-implanted Si to monitor the diffusion behavior resulting from the excess self-interstitials,<sup>11</sup> TEM experiments were conducted to observe the consequential defect structure using similar methodology;<sup>12-14</sup> conversely, the defect morphology of ion-implanted Si<sub>1-x</sub>Ge<sub>x</sub> alloys remains unclear. Defect analysis of ion irradiated, relaxed Si<sub>1-x</sub>Ge<sub>x</sub> alloys will supply valuable knowledge about the behavior and migration of dopants in Si<sub>1-x</sub>Ge<sub>x</sub>. This article will investigate the subsequent defect structure caused by the

excess interstitials present after Si implantation and annealing.

## II. EXPERIMENTAL DESIGN

Relaxed Si<sub>1-x</sub>Ge<sub>x</sub> wafers were grown by molecular beam epitaxy. Investigated Ge contents were 0%, 2%, 5%, 25%, and 50%. The pure Si sample was grown by the “bottle-neck” method to getter contaminants from the epitaxially grown top layer. Ge was incorporated into the other samples using a compositionally graded buffer layer. At an increasing rate of 10% Ge/μm and high growth temperatures around 750–800 °C, the relaxed alloys were grown. The samples with Ge were also lightly doped ( $5 \times 10^{15} \text{ cm}^{-3}$ ) with Sb. The top layers of constant composition ranged between 3 and 4 μm in thickness. The samples underwent a 40 keV,  $1 \times 10^{14} \text{ cm}^{-2}$  nonamorphizing Si implant, and then they were thinned for plan-view transmission electron microscopy (PTEM). A N<sub>2</sub> tube furnace tube was utilized to anneal the samples for 3 h at 750 °C in distinct intervals. PTEM using a JEOL 200CX microscope was conducted under weak beam, dark-field ( $g_{220}$ ) imaging conditions. Loop density, {311} defect density, and {311} defect size were measured to determine the relationship between defect evolution and Ge content.

## III. RESULTS

To highlight the dissimilarity in resulting defect structure from the various Ge concentrations, the work has been divided into two regimes: the low Ge concentration samples (pure Si, Si<sub>0.98</sub>Ge<sub>0.02</sub>, and Si<sub>0.95</sub>Ge<sub>0.05</sub>) and the high Ge concentration samples (Si<sub>0.75</sub>Ge<sub>0.25</sub> and Si<sub>0.50</sub>Ge<sub>0.50</sub>). Within 20–30 min, distinct {311} defects begin to form in the low Ge concentrated samples. Figures 1(a)–1(d) PTEM images of the defect morphology resulting from a 750 °C anneal of Si-implanted Si<sub>0.98</sub>Ge<sub>0.02</sub> illustrate this trend. At 30 min, {311} defects are evident with a few dislocation loops. Fif-

<sup>a)</sup>Electronic mail: rcros@mse.ufl.edu

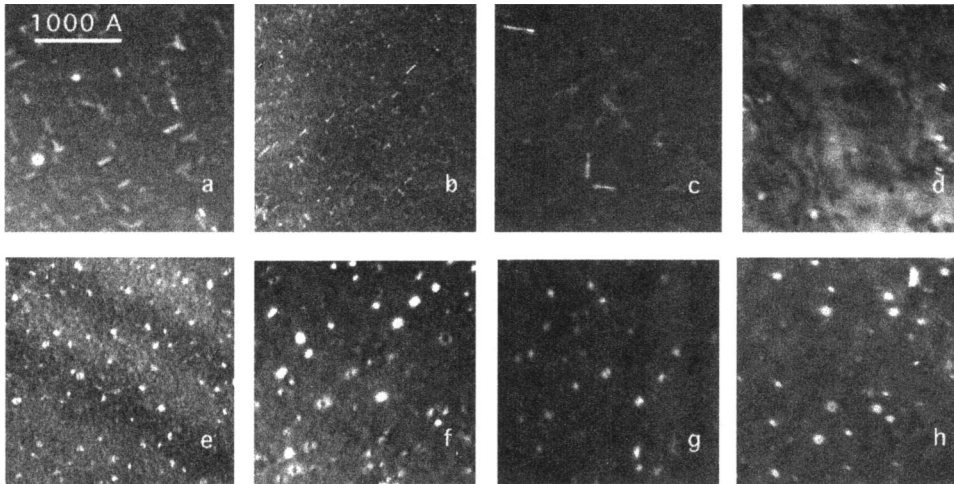


FIG. 1. PTEM images of 40 keV,  $1 \times 10^{14} \text{ cm}^{-2}$  Si implant into relaxed  $\text{Si}_{0.98}\text{Ge}_{0.02}$  [(a) 30 min, (b) 45 min, (c) 60 min, and (d) 120 min] and  $\text{Si}_{0.75}\text{Ge}_{0.25}$  [(e) 30 min, (f) 45 min, (g) 60 min, and (h) 120 min] annealed at  $750^\circ\text{C}$ .

teen min later, the {311} defects have increased in number. From 30 to 60 min, the {311} defects have grown in size and decreased in number. As time progresses even further, the number of {311} defects continues to decrease while the number of dislocation loops increases. Small stacking faults are also seen after 120 min of annealing, but are no longer visible in micrographs following 120 min.

Figures 1(e)–1(h) show the defect evolution of  $\text{Si}_{0.75}\text{Ge}_{0.25}$ . At 30 min, apparent dislocation loops form. At 45 min, the size of the dislocation loops appears to increase and then decrease at 60 and 120 min. The micrographs reveal that the size of the loops changes; however, the density of dislocation loops appears to remain the same throughout the anneal. Another figure to note is that only dislocation loops are observed in the high Ge content regime samples.

The ripening of {311} defects for the low Ge content regime samples is indicated by Figs. 2(a)–2(c). Coarsening of {311} defects is highly dependent upon Ge content. The density of {311} defects decreases over time while the size increases for all alloys. Figures 3(a) and 3(b) illustrate the {311} defect density and size for all of the low Ge regime alloys, respectively. The rate at which the density of {311} defects decays seems to be fairly independent of Ge concentration. Conversely, Ge concentration seems to have a profound effect on the size of the defects. Approximately at 45 min, the {311} defects in all samples grow to about 13 nm for all samples. By 120 min, the {311} defects are longest ( $\sim 55$  nm) for pure Si and shortest ( $\sim 18$  nm) for the  $\text{Si}_{0.95}\text{Ge}_{0.05}$ . Ripening of {311} defects is thus hindered by Ge incorporation.

The dislocation loop density of the high Ge content regime samples is specified in Fig. 4. For these samples, no {311} defects were detected; only dislocation loops evolved. Dislocation loops decomposed faster in the  $\text{Si}_{0.50}\text{Ge}_{0.50}$  alloy therefore exhibiting a more distinct dissolution of these defects. At about 120 min, stacking faults were detected in the  $\text{Si}_{0.50}\text{Ge}_{0.50}$  alloy as well. Dislocation loop formation appears to stabilize in the  $\text{Si}_{0.75}\text{Ge}_{0.25}$  alloy. Nevertheless, it is intriguing that increasing Ge content favors loop formation over {311} defect formation.

Dislocation loops are known to follow from the decomposition of {311} defects.<sup>9</sup> These findings suggest that increasing Ge content of  $\text{Si}_{1-x}\text{Ge}_x$  alloys seems to encourage dislocation loop formation. Adding Ge to the alloy either accelerates the unfauling of {311} defects or the excess in-

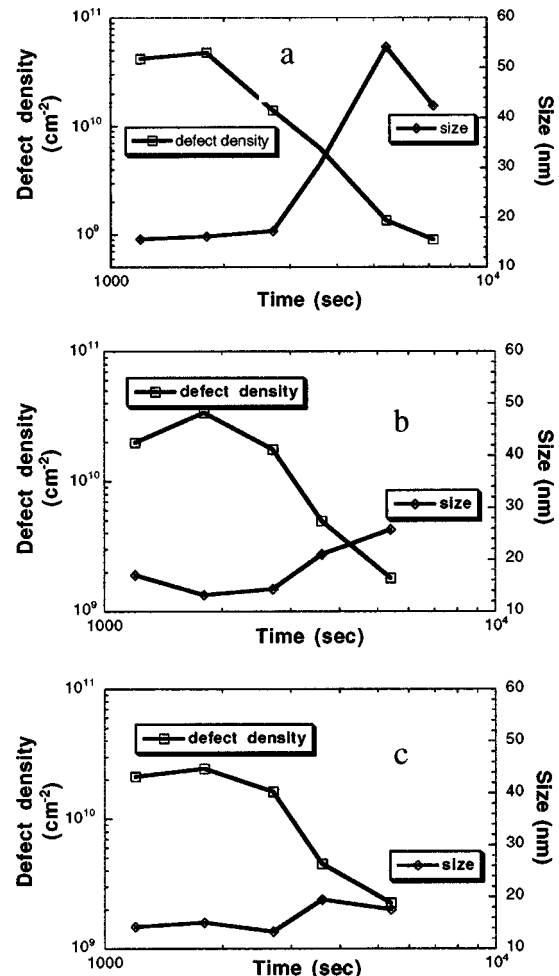


FIG. 2. {311} defect density and size of the low Ge regime alloys, (a) pure Si, (b)  $\text{Si}_{0.98}\text{Ge}_{0.02}$ , and (c)  $\text{Si}_{0.95}\text{Ge}_{0.05}$ , annealed at  $750^\circ\text{C}$ .

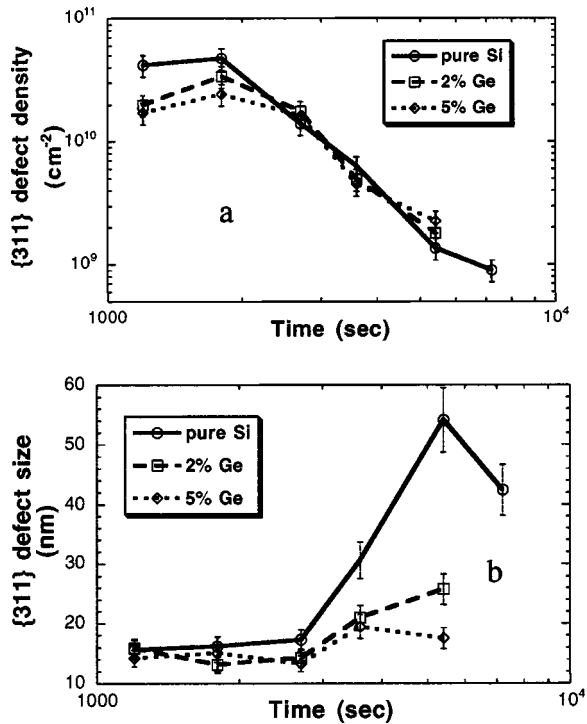


FIG. 3. (a) {311} defect density and (b) {311} defect size of the low Ge regime alloys annealed at 750 °C.

terstitials precipitate immediately into dislocation loops thus skipping {311} defect formation altogether. Increasing Ge concentration also impedes the ensuing ripening of {311} defects in the low Ge regime alloys. The high bonding energy

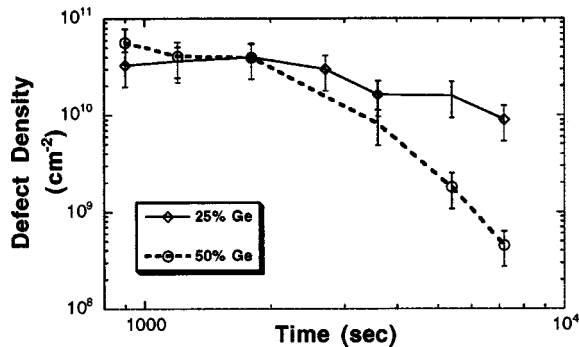


FIG. 4. Dislocation loop density of the high Ge regime alloys annealed at 750 °C.

(~1 eV/bond) associated with the covalent bonding of Si supports the formation of the {311} defect.<sup>8</sup> Adding larger, less rigid Ge atoms to the alloy lowers the overall bond energy and may generate strain in the system that would encourage the formation of dislocation loops instead of {311} defects.

#### IV. DISCUSSION

In summary, the defect morphology of Si-implanted relaxed Si<sub>1-x</sub>Ge<sub>x</sub> alloys depends on Ge concentration. With the pure Si, Si<sub>0.98</sub>Ge<sub>0.02</sub>, and Si<sub>0.95</sub>Ge<sub>0.05</sub> alloys, distinct {311} defects are observed within 30 min of annealing. The coarsening of the {311} defects is hindered with increasing Ge content. The density of {311} defects seems to decay independently of Ge content. For the intermediate Ge concentrated alloy Si<sub>0.75</sub>Ge<sub>0.25</sub>, dislocation loops appear relatively stable. When Ge content is increased to 50%, the dislocation loops become unstable.

#### ACKNOWLEDGMENTS

The authors would like to extend gratitude to Jackie Frazer for TEM sample preparation, the SWAMP Group, and the NSF and SRC for their support. The authors would also like to acknowledge Varian Semiconductors for their support.

- <sup>1</sup>S. Iyer, G. Patton, S. Delage, S. Tiwari, and J. Stork, Proceedings of the Si-MBE Symposium, 1987 (unpublished), p. 114.
- <sup>2</sup>C. A. King, J. L. Hoyt, C. M. Gronet, J. F. Gibbons, M. P. Scott, and J. Turner, IEEE Electron Device Lett. **EDL-10**, 52 (1989).
- <sup>3</sup>R. People, IEEE J. Quantum Electron. **QE-22**, 1696 (1986).
- <sup>4</sup>G. L. Patton, J. H. Comfort, B. S. Meyerson, E. F. Crabbe, G. J. Scilla, E. De Fresart, J. C. Stork, J. Y.-C. Sun, D. L. Harne, and J. N. Burghartz, IEEE Electron Device Lett. **11**, 171 (1990).
- <sup>5</sup>D. J. Eagelsham, P. A. Stolk, H.-J. Gossmann, and J. M. Poate, Appl. Phys. Lett. **65**, 2305 (1994).
- <sup>6</sup>W. Vandervorst, D. C. Houghton, F. R. Shepherd, M. L. Swanson, H. H. Plattner, and G. J. C. Carpenter, Can. J. Phys. **63**, 863 (1985).
- <sup>7</sup>K. S. Jones, S. Prussin, and E. R. Weber, Appl. Phys. A: Solids Surf. **45**, 1 (1988).
- <sup>8</sup>T. Y. Tan, Philos. Mag. A **44**, 101 (1981).
- <sup>9</sup>J. Li and K. S. Jones, Appl. Phys. Lett. **73**, 3748 (1998).
- <sup>10</sup>C. S. Rafferty, G. H. Gilmer, M. Jaraiz, D. Eaglesham, and H.-J. Gossmann, Appl. Phys. Lett. **68**, 2395 (1996).
- <sup>11</sup>P. Packan, Ph.D. thesis, Stanford University, 1991.
- <sup>12</sup>J. L. Benton, S. Libertino, P. Kringhoj, D. C. Jacobson, J. M. Poate, and S. Coffa, J. Appl. Phys. **81**, 120 (1997).
- <sup>13</sup>L. S. Robertson, K. S. Jones, L. M. Rubin, and J. Jackson, J. Appl. Phys. **87**, 2910 (2000).
- <sup>14</sup>H. Saleh, M. E. Law, S. Bharatan, K. S. Jones, V. Krishnamoorthy, and T. Buyuklimanli, Appl. Phys. Lett. **77**, 112 (2000).